Available online at www.sciencedirect.com
SCIENCE DIRECT®
European Journal of Medicinal Chemistry 41 (2006) 296–305
EUROPEAN JOURNAL OF MEDICINAL CHEMISTRY
http://france.elsevier.com/direct/ejmech

Original article

Synthesis of 3-substituted-2-oxoindole analogues and their evaluation as kinase inhibitors, anticancer and antiangiogenic agents

Ashraf H. Abadi [a,*], Sahar M. Abou-Seri [a], Doaa E. Abdel-Rahman [a], Christian Klein [b], Olivier Lozach [c], Laurent Meijer [c]

[a] *Department of Pharmaceutical Chemistry, Faculty of Pharmacy, Cairo University, Kasr El-Aini street, Cairo 11562, Egypt*
[b] *Pharmaceutical and Medicinal Chemistry, Saarland University, P.O. Box 151150, D-66041 Saarbrücken, Germany*
[c] *CNRS, Station Biologique, BP 74, 29682 Roscoff cedex, France*

Received 31 August 2005; received in revised form 17 November 2005; accepted 5 December 2005
Available online 21 February 2006

Abstract

Several analogues of the 3-substituted-2-oxoindole chemotype were synthesized by condensing isatin or the appropriate haloisatin with some amino acids or histamine under neutral conditions. All the imino derivatives produced were tested for kinase inhibitory properties against three serine/threonine kinases, namely CDK1/cyclin B, CDK5/p25 and GSK3α/β. Most of the histidine derivatives showed inhibitory properties to the three kinases in the low micromolar range. The histamine derivatives were less potent against CDK1/cyclin B and CDK5/p25 and totally inactive against GSK3α/β. So, the management of the carboxyl function may be a tool to impart selectivity in such family of kinases. Docking of 2-{[-5-bromo-2-oxoindolin-3-ylidene]amino}-3-(1*H*-imidazol2-yl)propanoic acid **14** to CDK5/p25 indicates that this compound can interact with the enzyme through four hydrogen bonds; for GSK/3β, the ligand poses itself in another orientation, also four hydrogen bonds can be formed between the ligand and the receptor, otherwise hydrophobic interactions seem to predominate. Also, all the final compounds were tested for their in vitro antitumor properties against MCF7 (breast), NCI-H460 (lung) and SF268 (CNS) cancer cell lines. None of the synthesized compounds was cytotoxic at 10^{-4} molar concentration. Moreover, compounds **13** and **14** were tested for potential antiangiogenic properties by testing their ability to inhibit the proliferation of human umbilical vein endothelial cells (HUVECs), cord formation and migration in response to chemoattractant. Only compound **14** showed moderate inhibitory properties to HUVECs proliferation and cord formation while its non-brominated derivative **13** did not. Thus, the antiangiogenesis properties are not apparently caused by inhibition of any of the tested kinases.

Keywords: Indolinone; Kinase inhibitors

1. Introduction

Protein phosphorylation on serine, threonine and tyrosine residues of proteins, using adenosine triphosphate (ATP) or guanosine 5′-triphosphate (GTP) as the phosphate donor, is considered to be one of the main post translational mechanisms used by cells to finely tune their metabolic and regulatory pathways [1,2]. Abnormal phosphorylation turns out to be a cause or consequence of numerous human diseases such as cancer, Alzheimer's disease, diabetes and atherosclerosis [3,4]. Excessive activity of cyclin-dependent kinases (CDKs) or aberrant functions of other kinases has been observed as one of the mechanisms underlying pathological hyperproliferation [5]. Consequently, inhibition of CDKs may be a therapeutic option for fighting tumor diseases [6,7]. In addition, since tumor growth and metastasis are angiogenesis dependent, microvascular endothelial cells recruited by a tumor have become an important target in cancer therapy [8]. Recent studies have shown a correlation between the blockade of different growth factors, inhibition of kinases and the inhibition of endothelial cell proliferation and angiogenesis [9,10]. Moreover, CDK5/p25 and GSK/3β are some of the most physiologically relevant kinases involved in the hyperphosporylation of the microtubule-binding

* Corresponding author. Tel.: +20 2 700 1507; fax: +20 2 362 8426.
E-mail address: ahabadi@yahoo.com (A.H. Abadi).

0223-5234/$ - see front matter © 2006 Elsevier SAS. All rights reserved.
doi:10.1016/j.ejmech.2005.12.004

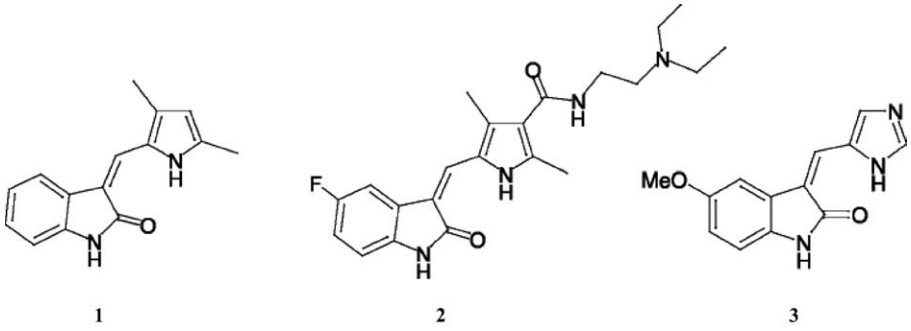

Fig. 1. Chemical structure of some 2-indolone derivatives that came into clinical trials as anticancer agents viz, SU-5416, Semaxanib **1**; SU-11248 **2**, Sunitinib; and SU-9516 **3**.

protein tau and beta-amyloid peptide production, two features observed in the brains of patients with Alzheimer's disease and other neurodegenerative 'taupathies' [11,12]. Also, the accumulation of p25 and increase of CDK5 activity in Alzheimer's disease patients brains, indicate that CDK5 activation may be involved in cytoskeletal abnormalities and neuronal death observed in those patients [13]. Since GSK-3 is phylogenetically closely related to CDKs, it is not surprising that several kinase inhibitor classes have dual activity [14].

Significant interest in the 2-oxoindoles derivatives as kinase inhibitors came after the disclosure of the tyrosine kinase inhibitory properties and antiangiogenesis properties of SU-5416 (semaxanib, **1)** [15–17] and SU-11248 (Sunitinib, **2)** Fig. 1, the latter molecule has recently completed phase III clinical trials with success. On the other hand, the structurally relevant SU9516 **(3)** was reported as potential CDKs inhibitor that induces apoptosis in colon carcinoma cells [18]. Moreover, indolinones with dual receptor tyrosine kinase and cyclin/CDK complex inhibitory properties has been reported for the treatment of endothelial cells and tumor cell proliferation [19]. In addition, CDK inhibitory properties has been reported to some isatin derived phenylhydrazones [37] and the structurally relevant indirubins [1].

Herein, we report upon the synthesis, kinase inhibitory properties, in vitro antitumor, and antiangiogenic properties of some 2-indolone imino derivatives obtained by the condensation of isatin or haloisatin with some amino acids and histamine.

2. Chemistry

The preparation of the target compounds **9–14** and **19–25** is depicted in Schemes 1–3. Briefly, isatin **4** and 5-bromoisatin **5** were refluxed with amino acids, namely valine **6,** threonine **7** and histidine **8,** under neutral conditions, to give the corresponding imino derivatives **9–14** in good yields. Derived by interactive SAR concept, derivatives **19–22** from chloroisatins **15–18** with the histidine aminoacid **8** were prepared (Scheme 2). The chloroisatins **15–18** were prepared by reported procedures, involving condensation of the appropriate chloroaniline with chloral hydrate and hydroxylamine to give the corresponding isonitrosoacetanilides followed by cyclization with sulfuric acid. The use of *m*-chloroaniline results in a mixture of 4- and 6-chloroisatin that was separated based upon the fractional decantation of the corresponding isatin sodium salts with acetic acid or hydrochloric acid [1,20]. Moreover, condensation of **4**, **5** and **16** with histamine yielded the imino derivatives **23–25**, Scheme 3.

Despite the fact that the condensation between isatin and *N*-unsubstituted-amino acids has been investigated before, little attention has been given to the characterization of the corresponding imino derivatives themselves or their stereochemistry, rather a characterization to their metal complexes or their complexes ionization properties has been studied [21–25]. Also, the products of the reaction of amino acids with isatin were controversial, whereas some authors reported the formation of the corresponding intact imines as in our case [21–24], others reported the formation of the corresponding imines with concomitant formation of the decarboxylated azomethine ylide through Strecker degradation [25,26].

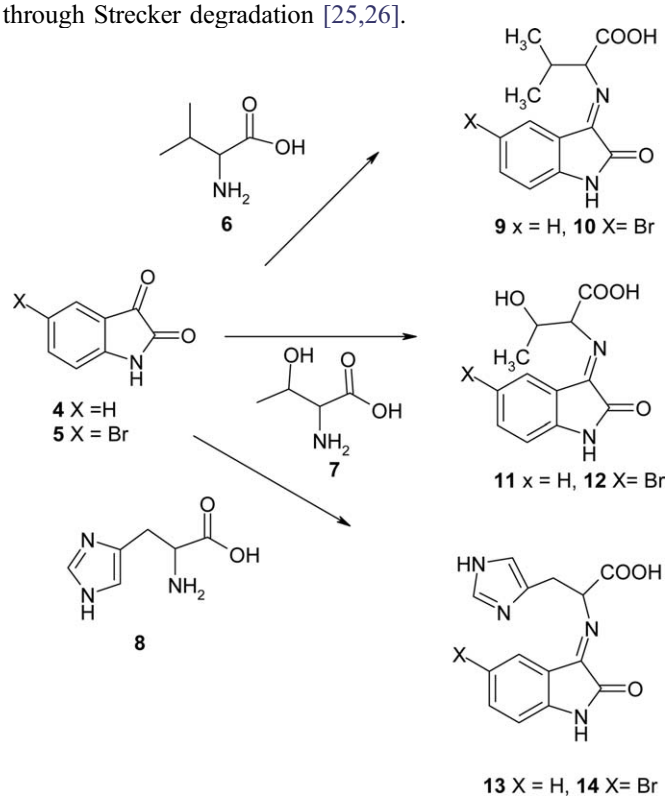

Scheme 1.

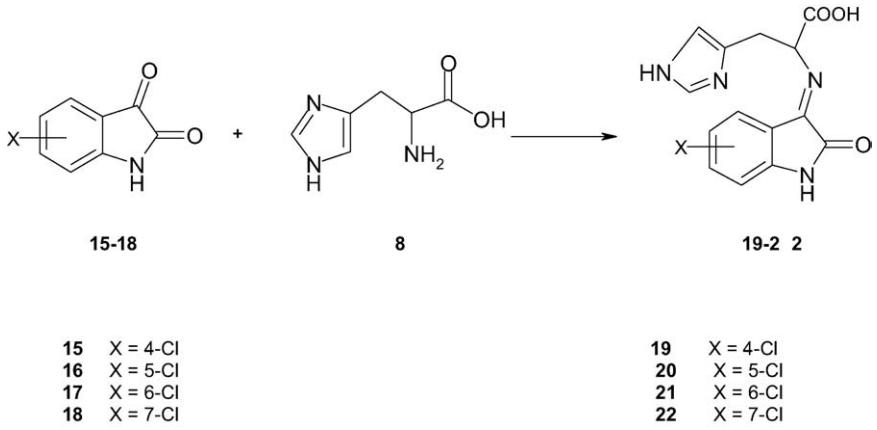

Scheme 2.

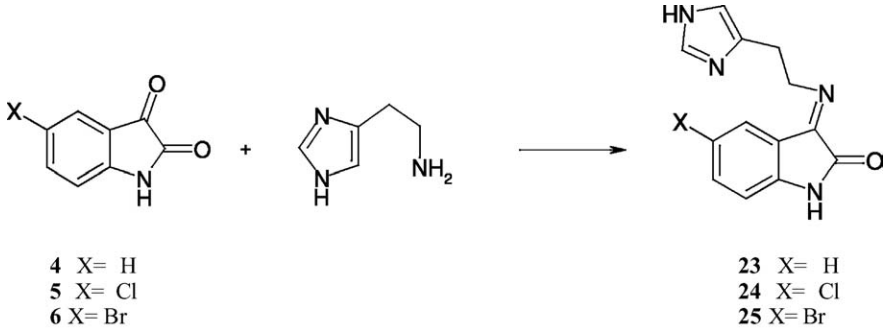

Scheme 3.

Trials to detect the molecular ion peaks of the amino acid imine derivative by electron impact mass spectrometry (EIMS) were difficult due to a weak or non-existing molecular ion peak, instead an ion peak at $[M-45]^+$ has been recognized, since these amino acids derivatives easily lose their carboxyl group upon electron impact [27]. A switch to chemical ionization mass spectrometry (CIMS) with methane gas as the ionizing reagent makes the molecular ion peaks often more prominent, moreover $[M + CH_3]^+$ adduct ion peaks were abundant, thus providing a higher degree of specificity for identification. The presence of a chlorine and a bromine atom in some imines leads to the formation of isotopic peaks at M^+ and $M^+ + 2$ in a 3:1 and 1:1 ratios, respectively. For the histamine derivatives **23–25** GC-EIMS was satisfactory to recognize the molecular ion peak.

The 3-substituted indolin-2-one may exist as either the *Z* or *E* isomer depending on the characteristics of the substituents at the C-3 position of the 3-substituted indolin-2-one and the nature of the substituent on position 4 of the indolinone core [28–30].

In our case, the GC/CIMS and GC/EIMS spectra of all the compounds except that of **19** showed them to be pure geometric isomers. The spectra of **19** showed two compounds in a nearly 1:1 ratio and with the same molecular ion peak and fragmentation pattern. This supports the hypothesis that the formation of the *E*-isomer seems to predominate in all cases except in that of compound **19**, whereby the 4-chloro substituent forces the position 3 indolinone substituent to attain the Z configuration by virtue of steric interference. In addition, conformational search did not generate any conformers with an intramolecular hydrogen bond between the imidazole and the indolinone rings, this bonding should enhance the formation of the *Z* isomer. This is due to the fact that the two ring systems are connected by a number of sp3-hybridized carbon atoms, which are not likely to adopt an eclipsed or nearly eclipsed conformation, that in turn, would be needed for the formation of a reasonably strong intramolecular hydrogen bond. This stands in contrast to compounds **1** [28], where the hydrogen-bond donor and acceptor atoms are connected by an sp2 hybridized carbon atom.

Moreover, the ^{1}H-NMR of the histidine and histamine derivatives **13**, **14**, **19–25** showed a clear upfield shift in the imidazole C-2 proton that appeared at < 7.55 ppm from the expected 7.74–9.00 ppm [31–33], such shielding action can only be attained with the imines in the *E*-configuration and the imidazole C-2 proton within the shielding cone of the phenyl ring of the 2-indolinone core (Fig. 2), this further confirms the existence of most of our derivatives in the *E*-configuration.

The ^{1}H-NMR spectra of the histamine imines **23–25** showed the ethylene protons as three or four multiplets rather than the expected two triplets, this indicates these molecules exist in more than one conformer, mostly the gauche–trans ones, such a remark has been previously reported in [33,34].

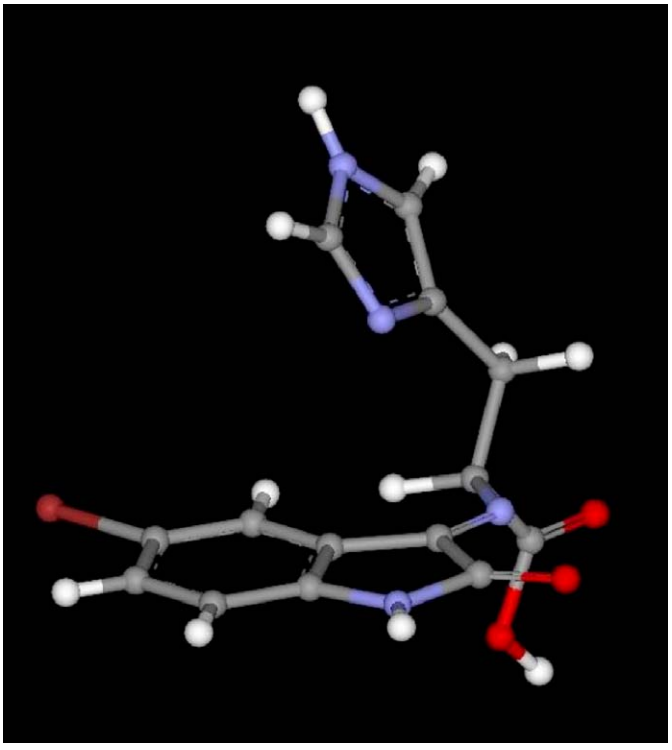

Fig. 2. Energy minimized form of the compound **14**, in the *E* configuration with the imidazole C-2 H within the shielding cone of the indolinone core.

3. Biological results and discussion

3.1. In vitro kinase inhibitory properties

First, all the final compounds shown in Scheme 1 **9–14** were tested for their potential inhibitory effect on three protein kinases, namely CDK1/cyclin B, CDK5/p25 and GSK-3α/β [1,35,36]. All the assays were run in the presence of 15 M ATP and appropriate protein substrates (histone H1 for CDKs, GS-1 peptide for GSK-3). The results are given in Table 1. Derivatives with valine and threonine amino acids **9–12** were inactive. Interestingly, the derivative with the isatin/histidine **13** was found to be active with IC_{50} values of 11, 2.5 and 15 M against CDK1/cyclin B, CDK5/p25 and GSK-3α/β, respectively. Moreover, the imine obtained from 5-bromoisatin and histidine **14**, was more potent than its non-brominated derivative against CDK1/cyclin B, CDK5/p25 and GSK-3α/β by factors of 10-fold, sevenfold and fivefold, respectively, Table 1. This may be due to better interaction with the kinase, because the binding pockets in these kinases are lined with mostly hydrophobic amino acids. Such a result encourages us to attempt further structural variations with the histidine amino acid. Derivatives with chlorine substituents at positions 4, 5, 6 and 7 of the indolinone ring (**19–22**; Scheme 2), were thus synthesized and tested for their kinase inhibitory properties. In addition to the electron withdrawing and hydrophobic properties that the chlorine substitution is expected to impart, the latter modification may block the oxidation of the indolone and may increase the metabolic stability of this class of compounds [18,19]. Three of the four chloro derivatives were found to be active against the three kinases, with the 5-chloro derivative **20** being the most potent with IC_{50} values of 1.0, 1.6 and 5.4 M against CDK1/cyclin B, CDK5/p25 and GSK-3α/β, respectively. Compound **20** was nearly 10 times more potent against CDK1/cyclin B and nearly three times as potent against GSK-3α/β compared to the non-halogenated derivative **13**. For those active derivatives, the order of potency was 5-chloro>6chloro>4-chloro against all three kinases. This confirms the positive impact of halogen substituents and highlights the importance of its position upon potency, with positions 5 and 6 being most optimal.

Table 1
Effects of the final imines upon various kinases

Compounds	IC_{50} (μM)[a]		
	CDK1/cyclinB	CDK5/p25	GSK3α/β
9	>100	>100	>100
10	>100	>100	>100
11	>100	>100	>100
12	>100	>100	>100
13	11	2.5	15
14	1.1	0.37	2.8
19	9.1	7.9	14
20	1.0	1.6	5.4
21	3.8	5.6	6.0
22	>100	>100	>100
23	>100	>100	>100
24	14	4.8	>100
25	50.0	13.0	>100

[a] Calculated from dose–response curves, obtained from the average of at least two experiments in triplicate.

For the inhibitory action of 4, 5 and 6-substituted haloisatins and the inactivity of the 7-substituted one, a previous report with other structurally related indolinone derivatives and CDK2 that differs from CDK1 only by two amino acids in the ATP binding pocket, showed the same favorable inhibitory pattern with a methyl substituent on position 4, 5 or 6 of the indolinone but not 7 as the substituent on position 7 pumps into the gate keeper and a similar effect would be expected with the chlorine substituent [37]. Moreover, we tested the impact of the carboxylic function upon kinase inhibition by preparing the decarboxylated analogues of **13**, **14** and **20**, viz compounds **23–25**. All the decarboxylated derivatives were less potent or totally inactive relative to their carboxylated analogues, highlighting the impact of the carboxylic function upon the inhibition of the kinases. The 5-halogenated decarboxylated derivatives **24** and **25** were still more potent than the dehalogenated decarboxylated corresponding analogue **23** against CDK1/cyclin B and CDK5/p25, the latter was totally inactive against the three kinases, thus confirming the positive effect of the 5-position halo derivative upon potency. Interestingly, all the decarboxylated analogues were totally inactive against GSK3α/β, this highlights the relevance of the carboxyl function as a tool to impart selectivity within this family of kinase (Table 1).

3.2. Molecular modeling

To further explore the mechanism of interaction between the active derivatives and different kinases, namely CDK5/p25 and GSK/3β a docking analysis was carried out. Conformational

search was done for compound **14** using the Macromodel software [38]. The lowest energy (potential energy of 281.6 kcal mol^{-1}) and the 11 other conformers within 8 kcal mol^{-1} of the energy minimum, showed no tendency for intramolecular hydrogen bond which, in theory, could be formed between the indolinone carbonyl oxygen and the imidazole ring.

To further explore the mechanism of interaction between the active derivatives and different kinases, namely CDK5/p25 and GSK/3β a docking analysis was carried out. The docked poses of **14** in CDK5/p25 and GSK are shown in Figs. 3 and 4, respectively. Fig. 3 illustrates the potential for four hydrogen bonds to CDK5/p25. Hydrogen bonds can be formed between the ligand carboxyl and the protein backbone and two H-bonds can be formed to amino acid side chains (ASP86 and ASN144). The bromine atom of the ligand is directed towards the entrance of the binding pocket in the CDK5/p25 structure. It interacts only partially with the phenyl ring of PHE82. The side chain of this residue is relatively flexible, which may explain the tolerance towards different substituents in the 5-position of the indolinone ligands. In the case of GSK/3β, the ligand is docked in the same orientation as found for bromoindirubine. The indolinone moieties of the two compounds are practically superimposable (Fig. 4). The carboxylic acid is exposed to the solvent and oriented towards GLN151 and makes a H-bond to the backbone carbonyl oxygen of that residue. The lack of this interaction may be responsible for the inactivity of the non-carboxylated congeners e.g. compound **24** versus compound **14** against GSK/3β. Also, compound **14** can form three more hydrogen-bonds, some of which are in analogy to the GSK-bromoindirubin X-ray structure, to the side chains of GLU103, VAL115, and ASP133 (pdb code 1UV5). Otherwise, hydrophobic interactions seem to dominate the binding of **14** to GSK3.

Moreover, the hydrophobic nature of the binding pocket may explain the higher potency of most of the bromine and

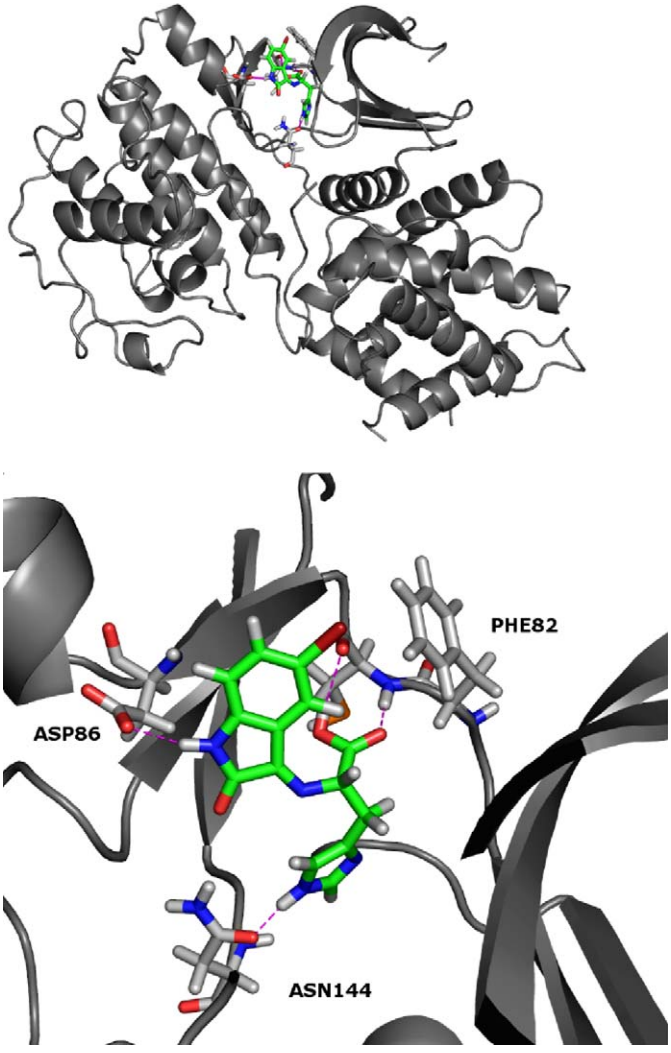

Fig. 3. Compound **14** docked in the ATP binding pocket of the catalytic site of CDK5/p25, mainly through hydrophobic interaction and four hydrogen bonds with PHE82, ASN144, ASP86 and CYS83. Overview (top) and close up of the active site (bottom). The ligand is shown in green.

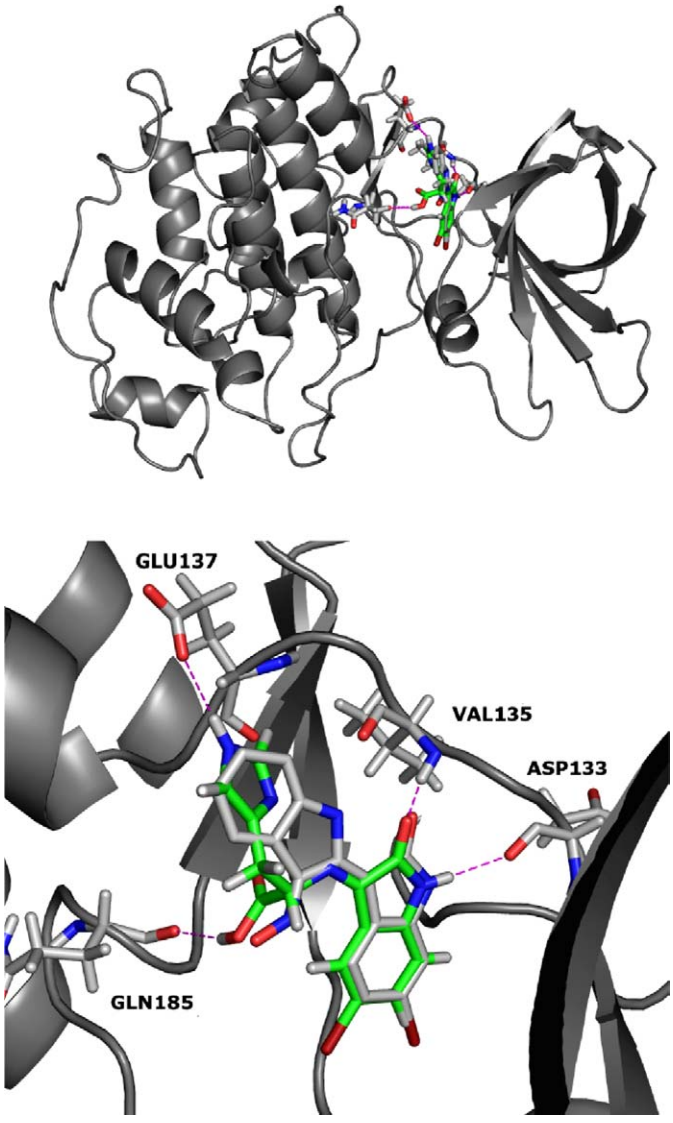

Fig. 4. Compound **14** docked into the ATP binding pocket of the catalytic site of GSK. Overview (top) and close up of the active site (bottom). Compound **14** is shown in green and bromoindirubine (from pdb 1UV5 crystal structure) is shown in gray.

chlorine derivatives as compared to the unsubstituted one as the binding cavities of CDK5/p25 and GSK/3β are lined mostly with hydrophobic amino acids.

3.3. In vitro antitumor testing [39,40]

All compounds were initially tested for cytotoxicity at a single 10^{-4} M concentration. This prescreen assay aims to eliminate a large proportion of the inactive agents, and preserve "active" agents for the multi-dose 60 cell line testing. Results for each compound are reported as the percent of growth of the treated cells when compared to the untreated control cells. Only compounds that reduce the growth of any of these cell lines to 32% or less are considered active and passed on for evaluation in the full six cell lines panel over a 5-log dose range. Cell lines in this prescreen were MCF7 Breast, NCI-H460 Lung and SF-268 CNS, as they are considered as good predictors of clinically useful drugs. All the final compounds **9–14** and **19–22** were evaluated in this prescreen test. As shown in Table 2, all the tested compounds were inactive. In this regard our compounds showed a behavior similar to that of compounds **1–3** [18,19]. One possible explanation for the lack of biological activity of compounds **9–14** and **19–25** is the presence of the acidic function which, by its charge, may prevent entry of the compounds into the cell.

3.4. Anti-angiogenesis testing

Angiogenesis is a complex process that includes endothelial cells proliferation, migration, alignment and formation of capillary like structures. Compounds **13** and **14** were selected for the anti-angiogenesis testing by the NCI. In particular, their ability to inhibit human umbilical vein endothelial cells (HUVECs) proliferation, cord formation and migration in response to chemoattractant [41,42] Although both compounds are kinase inhibitors, only compound **14** seems to be active at non-cytotoxic doses (Table 3). The inactivity of compound **13** indicates that the anti-angiogenic activity in this case is independent of their kinase inhibitory properties. Compound **14** inhibits endothelial cells proliferation rather than cord formation and chemotaxis in response to chemoattractants.

Table 2
Three cell panel, growth percentages after incubation with 10^{-4} M drug concentration

Compounds	(Breast) MCF7	(Non-small cell lung) NCI-H460	(CNS) SF-268
9	168	113	126
10	124	94	116
11	161	105	126
12	152	117	121
13	160	115	123
14	158	117	125
19	127	107	121
20	162	104	123
21	170	121	118
22	150	124	122
23	100	98	122
24	122	118	105
25	113	90	110

Table 3
The in vitro activities of some selected compounds upon HUVEC cells

Compounds	IC_{50} (μM)		
	Proliferation inhibition	Inhibition of cord formation	Inhibition of chemotaxis
13	>100	>100	>100
14	29	80	>100

In conclusion, we have generated imines composed of isatin or haloisatins coupled with histidine, and histamine as a new scaffold structure for protein kinase inhibition. The positive contribution of the halogen substituent particularly on positions 5 and 6 of the indolone moiety and of the carboxylic function may provide some interesting clues to improve the potency or selectivity of such class of compounds, respectively. The commercial availability of the starting materials, their diversity and the one step synthesis procedure add positively to this approach.

4. Experimental

4.1. Chemistry

Melting points were determined on the Electrothermal Melting Point apparatus and were uncorrected. Infrared spectra were recorded on the Shimadzu-470 infrared spectrophotometer. ^{1}H-NMR spectra were recorded in DMSO-d_6 on Varian XL-300 MHz spectrometers or varian XL200 MHz (chemical shifts are given in parts per million (PPM)). Elemental analyses (C, H, N) were performed by the Microanalytical Unit, Faculty of Science, Cairo University; the values were found to be within ±0.4% of the theoretical ones, unless otherwise indicated. Gas chromatography (GC) CIMS spectra were made on Finnigan MAT, SSQ 7000 while GC-EIMS were made on Hewlett Packard GC–MS, model 5890, series II. Intermediates **15–18** were prepared by a reported procedure [1,20].

4.1.1. General procedure for the synthesis of the final compounds *9–14* and *19–25*

A mixture of 0.01 mol of isatin or the appropriate haloisatin is refluxed with an equimolar amount of the appropriate neutral L-amino acid or histamine in ethanol (10 ml) for 5 hours and left to cool. The precipitated solid was filtered, washed with water, dried and crystallized from the appropriate solvent.

*4.1.1.1. 3-Methyl-2-{[2-oxoindolin-3-ylideneamino}butanoic acid (**9**).* Yield 58%; m.p. 106–108 °C; ethanol/ether; IR (KBr, cm^{-1}): 3400–2400, 3220, 2980, 1730, 1690, 1610; ^{1}H-NMR: 0.86–1.10 (m, 6H, 2 × CH_3), 2.05–2.14 (m, 1H, CH (CH_3)$_2$), 4.27 (d, 1H, CH–COOH), 6.76–7.45 (m, 4H, aromatic), 10.20 (brs, 1H, NH), 10.45 (brs, 1H, COOH); CIMS *m/z*: 246 (M^+, 5%); Anal. ($C_{13}H_{14}N_2O_3 \cdot 0.1H_2O$) C, H, N.

*4.1.1.2. 2-(5-Bromo-2-oxoindolin-3-ylideneamino)-3-methylbutanoic acid (**10**)*. Yield 70%; m.p. 137–139 °C; ethanol/ether; IR (KBr, cm^{-1}): 3400–2400, 3230, 2990, 1735, 1690, 1620; ^{1}H-NMR: 0.84–1.06 (m, 6H, 2 × CH_3), 1.92–2.08 (m, 1H, CH $(CH_3)_2$), 4.22 (d, 1H, CH–COOH, $J = 7$ Hz), 6.78–7.25 (m, 3H, aromatic), 10.20 (brs, 1H, NH), 10.40 (brs, 1H, COOH);; CIMS *m/z*: 326 (M^+), 328 ($M^+ + 2$); Anal. ($C_{13}H_{13}BrN_2O_3 \cdot 0.2H_2O$) C, H, N.

*4.1.1.3. 3-Hydroxy-2-{[-2-oxoindolin-3-ylidene]amino}butanoic acid (**11**)*. Yield 63%; m.p. 211–213 °C; ethanol/pet. ether; IR (KBr, cm^{-1}): 3400–2450, 3270, 2970, 1720, 1690, 1620; ^{1}H-NMR: 1.07–1.14 (m, 3H, CH_3), 3.57–3.60 (m, 1H, CH–CH_3), 4.08–4.17 (m, 1H, CH–COOH), 6.73–7.50 (m, 5H, aromatic, OH), 10.20 (brs, 1H, NH), 10.54 (brs, 1H, COOH); CIMS *m/z*: 248 (M^+, 16%); Anal. ($C_{12}H_{12}N_2O_4$) C, H, N.

*4.1.1.4. 2-{[-5-Bromo-2-oxoindolin-3-ylidene]amino}-3-hydroxybutanoic acid (**12**)*. Yield 58%; m.p. 158–159 °C; ethanol/pet. ether; IR (KBr, cm^{-1}): 3400–2500, 3250, 2950, 1720, 1690, 1615; ^{1}H-NMR: 1.03–1.24 (m, 3H, CH_3), 3.50–3.60 (m, 1H, CH–CH_3), 4.05–4.28 (m, 1H, CH–COOH), 6.73–7.51 (m, 4H, aromatic, OH), 9.80 (s, 1H, NH), 10.0 (brs, 1H, COOH); MS *m/z:* 328 (M^+), 330 ($M^+ + 2$); Anal. ($C_{12}H_{11}BrN_2O_4 \cdot 0.2H_2O$) C, H, N.

*4.1.1.5. (E)-3-(1H-imidazol-2-yl)-2-{[2-oxoindolin-3-ylidene]amino}propanoic acid (**13**)*. Yield 61%; m.p. 248–250 °C; ethanol/ether; IR (KBr, cm^{-1}): 3400–2400, 3200, 1720, 1690, 1610; ^{1}H-NMR: 3.45–3.49 (m, 2H, CH_2), 4.00–4.15 (m, 1H, CH–COOH), 6.67–7.48 (m, 6H, aromatic), 10.2 (brs, 1H, NH, exchangeable), 10.50 (brs, 1H, COOH, exchangeable), 11.80 (brs, 1H, NH, exchangeable); CIMS *m/z:* 284 (M^+, 13%); Anal. ($C_{14}H_{12}N_4O_3$) C, H, N.

*4.1.1.6. (E)-2-{[-5-bromo-2-oxoindolin-3-ylidene]amino}-3-(1H-imidazol-2-yl)propanoic acid (**14**)*. Yield 60%; m.p. 228–230 °C; ethanol/ether; IR (KBr, cm^{-1}): 3400–2400, 3200, 1720, 1680, 1620; ^{1}H-NMR: 3.43–3.48 (m, 2H, CH_2), 4.05–4.28 (m, 1H, CH–COOH), 6.76–7.54 (m, 5H, aromatic), 10.2 (brs, 1H, NH, exchangeable), 10.60 (brs, 1H, COOH, exchangeable), 12.2 (brs, 1H, NH, exchangeable); CIMS *m/z:* 364 (M^+), 366 ($M^+ + 2$); Anal. ($C_{14}H_{11}BrN_4O_3$) C, H, N.

*4.1.1.7. 2-{[4-Chloro-2-oxoindolin-3-ylidene]amino}-3-(1H-imidazol-2-yl)propanoic acid (**19**)*. Yield 57%; m.p. 191–193 °C; ethanol/ether; IR (KBr, cm^{-1}): 3400–2400, 3250, 1730, 1690, 1610; ^{1}H-NMR: 3.43–3.48 (m, 2H, CH_2), 4.05–4.28 (m, 1H, CH–COOH), 6.76–7.33 (m, 5H, aromatic), 10.35 (brs, 1H, NH, exchangeable), 10.61 (brs, 1H, COOH, exchangeable), 11.23 (brs, 1H, NH, exchangeable); CIMS *m/z*: 318 (M^+), 320 ($M^+ + 2$); Anal. ($C_{14}H_{11}ClN_4O_3$) C, H, N.

*4.1.1.8. (E)-2-{[5-chloro-2-oxoindolin-3-ylidene]amino}-3-(1H-imidazol-2-yl)propanoic acid (**20**)*. Yield 70%; m.p. 228–230 °C; ethanol/ether; IR (KBr, cm^{-1}): 3400–2400, 3230, 1720, 1690, 1620; ^{1}H-NMR: 3.50–3.53 (m, 2H, CH_2), 3.90–4.20 (m, 1H, CH–COOH), 6.78–7.50 (m, 5H, aromatic), 10.43 (brs, 1H, NH, exchangeable), 10.79 (brs, 1H, COOH, exchangeable), 11.78 (brs, 1H, NH, exchangeable); CIMS *m/z*: 318 (M^+), 320 ($M^+ + 2$); Anal. ($C_{14}H_{11}ClN_4O_3$) C, H, N.

*4.1.1.9. (E)-2-{[6-chloro-2-oxoindolin-3-ylidene]amino}-3-(1H-imidazol-2-yl)propanoic acid (**21**)*. Yield 67%; m.p. 200–202 °C; ethanol/ether; IR (KBr, cm^{-1}): 3400–2400, 3250, 1720, 1680, 1615 ^{1}H-NMR: 3.43–3.51 (m, 2H, CH_2), 4.00–4.20 (m, 1H, CH–COOH), 6.78–7.40 (m, 5H, aromatic), 10.2 (brs, 1H, NH, exchangeable), 10.45 (brs, 1H, COOH, exchangeable), 11.20 (brs, 1H, NH, exchangeable); CIMS *m/z*: 318 (M^+), 320 ($M^+ + 2$); Anal. ($C_{14}H_{11}ClN_4O_3$) C, H, N.

*4.1.1.10. (E)-2-{[7-chloro-2-oxoindolin-3-ylidene]amino}-3-(1H-imidazol-2-yl)propanoic acid (**22**)*. Yield 50%; m.p. 148–150 °C; ethanol/ether; IR (KBr, cm^{-1}): 3400–2400, 3250, 1730, 1690, 1620; ^{1}H-NMR: 3.40–3.42 (m, 2H, CH_2), 4.02–4.22 (m, 1H, CH–COOH), 6.80–7.42 (m, 5H, aromatic), 10.23 (brs, 1H, NH, exchangeable), 10.60 (brs, 1H, COOH, exchangeable), 11.80 (brs, 1H, NH, exchangeable); CIMS *m/z:* 318 (M^+), 320 ($M^+ + 2$); Anal. ($C_{14}H_{11}ClN_4O_3$) C, H, N.

*4.1.1.11. C;(E)-3-(2-(1H-imidazol-4-yl)ethylimino)indolin-2-one (**23**)*. Yield 56%; m.p. 268–270 °C; ethanol/ether; IR (KBr, cm^{-1}): 3300, 1700, 1620; ^{1}H-NMR: 2.562.76 (m, 2H, CH_2–CH_2–N), 3.04–3.06 (m, 1H, CH_2–CH_2–N), 3.46–3.54 (m, 1H, CH_2–CH_2–N); 6.80–7.30 (m, 6H, aromatic), 10.15 (s, 1H, NH, exchangeable), 11.78 (s, 1H, NH, exchangeable); EIMS: *m/z* 240 (M^+, 16%); Anal. ($C_{13}H_{12}N_4O$) C, H, N.

*4.1.1.12. (E)-3-(2-(1H-imidazol-4-yl)ethylimino)-5-chloroindolin-2-one (**24**)*. Yield 56%; m.p. 286–287 °C; ethanol/ether; IR (KBr, cm^{-1}): 3300, 1710, 1620; ^{1}H-NMR: 2.56–2.70 (m, 1H, CH_2–CH_2–N), 2.80–2.86 (m, 1H, CH_2–CH_2–N), 3.02–3.06 (m, 1H, CH_2–CH_2–N), 3.46–3.54 (m, 1H, CH_2–CH_2–N), 6.82–7.33 (m, 5H, aromatic), 10.29 (s, 1H, NH, exchangeable), 11.80 (s, 1H, NH, exchangeable); EIMS: *m/z* 274 (M^+), 276 ($M^+ + 2$); Anal. ($C_{13}H_{11}ClN_4O$) C, H, N.

*4.1.1.13. (E)-3-(2-(1H-imidazol-4-yl)ethylimino)-5-bromoindolin-2-one (**25**)*. Yield 75%; m.p. 276–277 °C; ethanol/ether; IR (KBr, cm^{-1}): 3350, 1700, 1620; ^{1}H-NMR: 2.59-2.71 (m, 2H, CH_2–CH_2–N), 3.02–3.06 (m, 1H, CH_2–CH_2–N), 3.46–3.50 (m, 1H, CH_2–CH_2–N), 6.78–7.36 (m, 5H, aromatic), 10.30 (brs, 1H, NH, exchangeable), 11.84 (brs, 1H, NH, exchangeable); EIMS: *m/z* 320 (M^+), 322 ($M^+ + 2$); Anal. ($C_{13}H_{11}BrN_4O$) C, H, N.

4.2. Kinase preparations and assays [1,35,36]

CDK1/cyclin B was extracted in homogenization buffer from M phase starfish (*Marthasterias glacialis*) oocytes and purified by affinity chromatography on p9CKShs1-sepharose beads, from which it was eluted by free p9CKShs1 as pre-

viously described in [35,36]. The kinase activity was assayed in buffer C, with 1 mg of histone H1 ml^{-1}, in the presence of 15 μM [γ^{-32}P]ATP (3000 Ci $mmol^{-1}$; 1 mCi ml^{-1}) in a final volume of 30 μl. After 10 min of incubation at 30 °C, 25 μl aliquots of supernatant were spotted onto 2.5 × 3-cm pieces of Whatman P81 phosphocellulose paper, and 20 s later, the filters were washed five times (for at least 5 min each time) in a solution of 10 ml of phosphoric acid l^{-1} of water. The wet filters were counted in the presence of 1 ml of ACS (Amersham) scintillation fluid.

CDK5/p25 was reconstituted by mixing equal amounts of recombinant mammalian CDK5 and p25 expressed in *E. coli* as glutathione-S-transferase (GST) fusion proteins and purified by affinity chromatography on glutathione agarose (vectors kindly provided by Dr. J. H. Wang) (p25 is a truncated version of p35, the 35 kDa CDK5 activator). Its activity was assayed in buffer C as described for CDK1/cyclin B (see above).

GSK-3α/β was purified from porcine brain by affinity chromatography on immobilized axin. It was assayed, following a 1/100 dilution in 1 mg of BSA ml^{-1} of 10 mM DTT, with 5 μl of 40 μM GS-1 peptide as a substrate, in buffer A, in the presence of 15 μM [γ^{-32}P] ATP (3000 Ci $mmol^{-1}$; 1 mCi ml^{-1}) in a final volume of 30 μl. After 30 min of incubation at 30 °C, 25 μl aliquots of supernatant were spotted onto 2.5 × 3-cm pieces of Whatman P81 phosphocellulose paper, and treated as under CDK1/cyclin B.

4.3. In vitro cytotoxicity assay [39,40]

4.3.1. Three cell lines prescreen

Briefly, the cancer-screening cell lines were grown in RPMI 1640 medium containing 5% fetal bovine serum and 2 mM L-glutamine. For a typical screening experiment, cells were inoculated into 96 well microtiter plates in 100 ml at plating densities ranging from 5000 to 40,000 cells per well depending on the doubling time of individual cell lines. After cell inoculation, the microtiter plates were incubated at 37 °C, 5% CO_2, 95% air and 100% relative humidity for 24 h prior to addition of experimental drugs. After 24 h, two plates of each cell line were fixed in situ with trichloroacetic acid (TCA), to represent a measurement of the cell population. For each cell line at the time of drug addition (Tz). Experimental drugs were solubilized in dimethyl sulfoxide at 400-fold the desired final maximum test concentration and stored frozen prior to use. At the time of drug addition, an aliquot of frozen concentrate was thawed and diluted to twice the desired final maximum test concentration with complete medium containing 50 mg ml^{-1} gentamicin. Aliquots of 100 μl of these different drug dilutions were added to the appropriate microtiter wells already containing 100 μl of medium, resulting in the required final drug concentrations. Following drug addition, the plates were incubated for an additional 48 h at 37 °C, 5% CO_2, 95% air, and 100% relative humidity. For adherent cells, the assay was terminated by the addition of cold TCA. Cells were fixed in situ by the gentle addition of 50 ml of cold 50% (w/v) TCA (final concentration, 10% TCA) and incubated for 60 min at 4 °C. The supernatant was discarded, and the plates were washed five times with tap water and air dried. Sulforhodamine B (SRB) solution (100 ml) at 0.4% (w/v) in 1% acetic acid was added to each well, and plates were incubated for 10 min at room temperature. After staining, unbound dye was removed by washing five times with 1% acetic acid and the plates were air dried. Bound stain is subsequently solubilized with 10 mM trizma base, and the absorbance was read on an automated plate reader at a wavelength of 515 nm.

4.4. Antiangiogenesis testings [41,42]

4.4.1. HUVEC cells growth inhibition assay

HUVEC (1.5×10^3) were plated in a 96-well plate in 100 μl of EBM-2 (Clonetic #CC3162). After 24 h (day 0), the test compound (100 μl) was added to each well at 2× the desired concentration (five to seven concentration levels) in EBM-2 medium. On day 0, one plate was stained with 0.5% crystal violet in 20% methanol for 10 min, rinsed with water, and air-dried. The remaining plates were incubated for 72 h at 37 °C. After 72 h, plates were stained with 0.5% crystal violet in 20% methanol, rinsed with water and air-dried. The stain was eluted with 1:1 solution of ethanol: 0.1 M sodium citrate (including day 0 plate), and absorbance was measured at 540 nm with an ELISA reader (Dynatech Laboratories). Day 0 absorbance was subtracted from the 72 h plates and data were plotted as percentage of control proliferation (vehicle treated cells). IC_{50} (drug concentration causing 50% inhibition) was calculated from the plotted data.

4.4.2. Cord formation assay

Matrigel (60 μl of 10 mg ml^{-1}; Collaborative Lab#35423) was placed in each well of an ice-cold 96-well plate. The plate was allowed to sit at room temperature for 15 min then incubated at 37 °C for 30 min to permit the matrigel to polymerize. In the mean time, HUVECs were prepared in EGM-2 (Clonetic #CC3162) at a concentration of 2×10^5 cells per ml. The test compound was prepared at 2× the desired concentration (five concentration levels) in the same medium. Cells (500 μl) and 2× drug (500 μl) was mixed and 200 μl of this suspension are placed in duplicate on the polymerized matrigel. After 24 h incubation, triplicate pictures were taken for each concentration using a Bioquant Image Analysis system. Drug effect (IC_{50}) was assessed compared to untreated controls by measuring the length of cords formed and number of junctions.

4.4.3. Cell migration assay

Migration was assessed using the 48-well Boyden chamber and 8 mm pore size collagen-coated (10 g ml^{-1} rat tail collagen; Collaborative Laboratories) polycarbonate filters (Osmonics, Inc.). The bottom chamber wells received 27–29 μl of DMEM medium alone (baseline) or medium containing chemoattractant VEGF 10 ng ml^{-1}. The top chambers received 45 μl of HUVEC cell suspension (1×10^6 cells ml^{-1}) prepared in DMEM11% BSA with or without test compound. After 5 h incubation at 37 °C, the membrane was rinsed in PBS, fixed

and stained in Diff-Quick solutions. The filter was placed on a glass slide with the migrated cells facing down and cells on top were removed using a Kimwipe. The testing was performed in four to six replicates and five fields were counted from each well. Negative unstimulated control values are subtracted from stimulated control and drug treated values and data were plotted as mean migrated cell ± S.D. IC_{50} is calculated from the plotted data.

4.5. Molecular modeling

4.5.1. Methods

4.5.1.1. Conformational search. The minimum conformer of compound **14** was determined using the MACROMODEL software [38] (csearch module, Monte Carlo Multiple Minimum method, MMFFs force field). All rotatable C–C and C–N bonds were flexible. 10000 Monte Carlo steps were taken. All conformers within 50 kcal mol^{-1} of the potential energy minimum were saved for further analysis.

4.5.1.2. Docking. The proteins (PDB ID code: 1UNL and 1UV5, for CDK5/p25 complexed with Roscovitine and GSK3/3β complexed with 6-bromoindirubin-3′-oxime, respectively) were prepared as follows: Upon removal of ions, water molecules and the co-crystallized ligands, the proteins were loaded into the xleap utility of AMBER-7 [43], where AMBER force field charges and hydrogen atoms were added. The proteins were then saved as amber OFF files and converted by in-house software to MOL2 files for use in the docking runs. A MOL2 files of the ligand was generated by Macromodel, followed by some minor manual changes (correction of aromatic carbons and aromatic bonds). The program GOLD was used to dock **14** into the binding sites of GSK and CDK5. The active site was defined from all residues within 10 Å of the center of the binding pocket. GOLD default settings without any speed-up were used for the docking, except that early termination was not allowed. Visualization was done using the Chimera [44] and PYMOL (NEW CITATION) [45] programs.

Acknowledgements

The authors are grateful to the National Cancer Institute (Bethesda, MD) for the antitumor and antiangiogenesis testing. This research was supported by the Ministère de la Recherche/Inserm/CNRS "Molécules et Cibles Thérapeutiques" Program (L.M.) and a grant from the EEC (FP6-2002-Life Sciences and Health, PRO-KINASE Research Project) (L.M.) and the Canceropole Grand Ouest.

References

[1] P. Polychronopoulos, P. Magiatis, A. Skaltsounis, V. Myrianthopoulos, E. Mikros, A. Tarricone, A. Musacchio, M. Roe, L. Pearl, M. Leost, P. Greengard, L. Meijer, J. Med. Chem. 47 (2004) 935–946.
[2] P. Cohen, Eur. J. Biochem. 268 (2001) 5001–5010.
[3] P. Cohen, Nat. Rev. Drug Discov. 1 (2002) 309–315.
[4] R. Sridhar, O. Hanson-Painton, D.R. Cooper, Pharm. Res. 17 (2000) 1345–1353.
[5] M. Malumbres, M. Barbacid, Nat. Rev. Cancer 1 (2001) 222–231.
[6] I.N. Roublevskaia, B.V. Polevoda, J.W. Ludlow, A.R. Haake, Anticancer Res. 20 (2000) 3163–3167.
[7] M. Knockaert, P. Greengard, L. Meijer, Trends Pharmacol. Sci. 23 (2002) 417–425.
[8] J. Folkman, J. Natl. Cancer Inst. 82 (1990) 4–6.
[9] H.C. Haspel, A.G. Scicli, G. McMahon, A. Guillermo Scicli, Microvasc. Res. 63 (2002) 304–315.
[10] T.A.T. Fong, L.K. Shawver, L. Sun, C. Tang, H. App, T.J. Powell, H. Y. Kim, R. Schreck, X. Wang, W. Risau, A. Ullrich, K.P. Hirth, G. McMahon, Cancer Res. 59 (1999) 99–106.
[11] B. De Strooper, J. Woodgett, Nature 423 (2003) 392–393.
[12] L. Meijer, M. Flajolet, P. Greengard, Trends Pharmacol. Sci. 25 (2004) 471–480.
[13] W. Noble, V. Olm, K. Takata, E. Casey, O. Mary, J. Meyerson, K. Gaynor, J. LaFrancois, L. Wang, T. Kondo, P. Davies, M. Burns, R. Veerana Nixon, D. Dickson, Y. Matsuoka, M. Ahlijanian, L.F. Lau, K. Duff, Neuron 38 (2003) 555–565.
[14] S. Leclerc, M. Garnier, R. Hoessel, D. Marko, J.A. Bibb, G.L. Snyder, P. Greengard, J. Biernat, E.-M. Mandelkow, G. Eisenbrand, L. Meijer, J. Biol. Chem. 276 (2001) 251–260.
[15] R.D. Connell, Expert Opin, Ther. Patents 13 (2003) 738–750.
[16] M.A. Jianguo, L.I. Shaolan, K. Reed, P. Guo, J.M. Gallo, J. Pharmcol. Exp. Ther. 305 (2003) 833–839.
[17] P. Marzola, A. Degrassi, L. Calderan, P. Farace, C. Crescimanno, E. Nicolato, A. Giusti, E. Pesenti, A. Terron, A. Sbarbati, T. Abrams, L. Murray, F. Osculati, Clin. Cancer Res. 15 (2004) 739–750.
[18] M.E. Lane, B. Yu, A. Rice, K.E. Lipson, C. Liang, L. Sun, C. Tang, G. McMahon, R.G. Pestell, S. Wadler, Cancer Res. 15 (2001) 6170–6177.
[19] G.J. Roth, A. Heckel, T. Lehmann-Lintz, J. Kley, F. Hilberg, J. Van Meel, Ger. Offen, 2002 (CODEN: GWXXBX DE 10117204 A1 20021010 CAN 137:279089 AN 2002:772126).
[20] R.J.H. Clark, C.J. Cooksey, J. Soc. Dyers Colour. 113 (1997) 316–321.
[21] A.M.A. Hassaan, E.M. Soliman, M.A. Sakran, Egypt. J. Pharm. Sci. 36 (1995) 309–320.
[22] A.M.A. Hassaan, Egypt. J. Pharm. Sci. 35 (1994) 165–171.
[23] A.M.A. Hassaan, A.M. El-Roudi, M.T.A. Quenawy, Egypt. J. Pharm. Sci. 34 (1993) 253–266.
[24] A.M.A. Hassaan, Egypt. J. Pharm. Sci. 33 (1992) 679–687.
[25] S. Rehn, J. Bergman, B. Stensland, Eur. J. Org. Chem. (2004) 413–418.
[26] M.F. Aly, G.M. El-Nagger, T.I. El-Emary, R. Grigg, S.A.M. Metwally, S. Sivagnanam, Tetrahedron 50 (1994) 895–906.
[27] G.W.A. Milne, T. Axenrod, H.M. Fales, J. Am. Chem. Soc. 92 (1970) 5170–5175.
[28] L. Sun, N. Tran, F. Tang, H. App, P. Hirth, G. McMahon, C. Tang, J. Med. Chem. 41 (1998) 2588–2603.
[29] L. Sun, N. Tran, C. Liang, F. Tang, A. Rice, R. Schreck, K. Waltz, L. K. Shawver, G. McMahon, C. Tang C. J. Med. Chem. 42 (1999) 5120–5130.
[30] A. Andreani, M. Granaiola, A. Leoni, A. Locatelli, R. Morigi, M. Rambaldi, V. Garaliene, J. Med. Chem. 45 (2002) 2666–2669.
[31] R. Ganellin, A. Fkyerat, B. Bang-Andersen, S. Athmani, W. Tertiuk, M. Garbarg, X. Ligneau, J. Schwatz, J. Med. Chem. 39 (1996) 3806–3813.
[32] S. GraBman, J. Apelt, W. Sippl, X. Ligneau, H.H. Pertz, Y.H. Zhao, J. Arrang, R. Ganellin, J. Schwartz, W. Schunacka, H. Stark, Bioorg. Med. Chem. 11 (2003) 2163–2174.
[33] N.S. Ham, A.F. Casy, R.R. Ison, J. Med. Chem. 16 (1973) 470–475.
[34] C.R. Ganellin, E.S. Pepper, J. Med. Chem. 16 (1973) 610–616.
[35] A. Primot, B. Baratte, M. Gompel, A. Borgne, S. Liabeuf, J.L. Romette, F. Costantini, L. Meijer, Protein Expr. Purif. 20 (2000) 394–404.
[36] A. Borgne, L. Meijer, J. Biol. Chem. 271 (1996) 27847–27854.
[37] H.N. Bramson, J. Corona, S.T. Davis, S.H. Dickerson, M. Edelstein, S. V. Frye, R.T. Gampe, P.A. Harris, A. Hassell, W.D. Holmes, R. N. Hunter, K.E. Lackey, B. Lovejoy, M.J. Luzzio, V. Montana, W. J. Rocque, D. Rusnak, L. Shewchuk, J.M. Veal, D.H. Walker, L. F. Kuyper, J. Med. Chem. 44 (2001) 4339–4358.

[38] F. Mohamadi, N.G.J. Richards, W.C. Guida, R. Liskamp, M. Lipton, C. Caufield, G. Chang, T. Hendrickson, W.C. Still, J. Comput. Chem. 11 (1990) 440–467.
[39] M.R. Greever, S.A. Schepartz, B.A. Chabner, Semin. Oncol. 19 (1992) 622–638.
[40] A. Monks, D. Scudiero, P. Dkehan, R. Shoemaker, K. Paull, D. Vistica, C. Hose, J. Langely, P. Cronise, M. Vaigro-Wolf, M. Gray-Good Rich, H. Campell, M.R. Mayo, J. Natl. Cancer Inst. 83 (1991) 757–766.
[41] G. Tarabolleti, G. Micheletti, M. Rieppi, M. Poli, M. Turatto, C. Rossi, P. Borsotti, P. Roccabianca, E. Scanziani, M.I. Nicoletti, E. Bombardelli, P. Morazzoni, A. Riva, R. Giavazzi, Clin. Cancer Res. 8 (2002) 1182–1188.
[42] D. Belotti, V. Vergani, T. Drudis, P. Borsotti, M.R. Pitelli, G. Viale, R. Giavazzi, G. Taraboletti Clin, Cancer Res. 2 (1996) 1843–1849.
[43] D.A. Case, D.A. Pearlman, J.W. Caldwell, T. E. C. III, J. Wang, University of California, San Francisco, 2002.
[44] C.C. Huang, G.S. Couch, E.F. Pettersen, T.E. Ferrin, Pacific Symposium on Biocomputing 1 (1996) 724.
[45] W.L. Delano, The PYMOL Molecular Graphics Sysyem (2002) http://www.pymol.org.